The EMBO Journal vol.14 no.6 pp.1084–1090, 1995

Structure and functional expression of a new member of the tetrodotoxin-sensitive voltage-activated sodium channel family from human neuroendocrine cells

Norbert Klugbauer, Lubica Lacinova[1], Veit Flockerzi[2] and Franz Hofmann[3]

Institut für Pharmakologie und Toxikologie der Technischen Universität München, Biedersteiner Straße 29, 80802 München, Germany
[2]Present address: Pharmakologisches Institut, Molekulare Pharmakologie, Im Neuenheimer Feld 366, 69120 Heidelberg, Germany
[1]On leave from the Institute for Molecular Physiology and Genetics, Vlarska 5, 83334 Bratislava, Slovakia

[3]Corresponding author

Communicated by B.Hamprecht

A member of a new subclass of the voltage-activated sodium channel genes has been cloned from the human medullary thyroid carcinoma (hMTC) cell line. The cDNA of hNE-Na (human neuroendocrine sodium channel) encodes a 1977 amino acid protein which phylogenetically represents a link between sodium channels isolated from skeletal muscle and brain. The hNE-Na α subunit was transiently expressed in human embryonic kidney cells either alone or in combination with the human sodium channel β1 subunit. The channel exhibited rapid activation and inactivation kinetics, and was blocked by tetrodotoxin and cadmium with IC_{50} values of 24.5 nM and 1.1 mM, respectively. Action potentials were generated in cells expressing high levels of hNE-Na. Northern blot and reverse transcription-polymerase chain reaction (RT-PCR) analyses demonstrated its expression in hMTC cells, in a C-cell carcinoma, and in thyroid and adrenal gland. Transcripts were not identified in pituitary gland, brain, heart, liver or kidney, indicating that the hNE-Na is a sodium channel solely expressed in neuroendocrine cells.

Key words: hMTC cells/neuroendocrine cell/sodium channel/tetrodotoxin

Introduction

Voltage-gated sodium channels are transmembrane proteins responsible for the propagation of the electrical signal in neurons, cardiac, skeletal muscle and neuroendocrine cells. The principal subunit of this channel is the α subunit, a protein of >200 kDa, which consists of four large domains of internal homology. The ion selectivity, voltage-dependent activation and inactivation, sensitivity to toxins, and the modulation by cAMP kinase and protein kinase C reside in the primary sequence of this subunit. Molecular cloning of the cDNA and site-directed mutagenesis of the α subunit have identified the amino acids responsible for the above properties [reviewed in Stühmer (1993) and Catterall (1994)]. The purified α subunit protein is associated with one or two additional proteins: the β1 and β2 subunits (reviewed in Isom *et al.*, 1994). The functional significance of these subunits is unclear. The β1 subunit speeded up inactivation and activation of sodium currents elicited by the expression of the rat brain II sodium channel in *Xenopus* oocytes in the experiments of some groups, but not in those of other groups (see Isom *et al.*, 1994). Co-expression of the β1 subunit with the α subunit in Chinese hamster ovary (CHO) or human embryonic kidney (HEK) cells did not significantly modify the resulting sodium current (West *et al.*, 1992).

The cloning of the cDNA of the voltage-dependent sodium channel led to the identification of seven different genes. Three genes are expressed in brain, two in skeletal muscle and two in the heart (Noda *et al.*, 1986; Kayano *et al.*, 1988; Trimmer *et al.*, 1989; Gellens *et al.*, 1992; George *et al.*, 1992). The brain sodium channels are expressed exclusively in the neurons of distinct brain regions (Beckh *et al.*, 1989). An additional molecular unidentified sodium channel may be present in certain glia cells (Gautron *et al.*, 1992). Voltage-dependent sodium channels have been identified in several neuroendocrine cells, which are derived from the neural crest (Fenwick *et al.*, 1982; Biagi *et al.*, 1992; Scherübl *et al.*, 1993). These cells include C-cells, chromaffine cells from the adrenal medulla and pheochromocytoma cells. The structure of these tetrodotoxin (TTX)-sensitive channels has not been elucidated, so far. Physiological experiments suggested that these sodium channels are involved in acetylcholine-triggered hormone release since they can generate an action potential, which leads to a voltage-dependent influx of calcium (Biales *et al.*, 1976; Scherübl *et al.*, 1993). We have used mRNA from the clonal C-cell line of a human medullary thyroid carcinoma (hMTC) cell line, which expressed a functional sodium channel in culture (Biagi *et al.*, 1992). The cloned and expressed human neuroendocrine sodium channel (hNE-Na) is a new member of the voltage-dependent sodium channel family, which is expressed exclusively in neuroendocrine cells and represents an evolutionary link between channels from brain and skeletal muscle.

Results

Primary structure of hNE-Na

The complete nucleotide sequence of hNE-Na consisted of an open reading frame of 5931 bp encoding a 1977 amino acid protein with a calculated molecular mass of 225 195 Da (Figure 1). The region directly upstream of the translational start site resembled the consensus sequence for eukaryotic initiation sites with an A base at position −3 and a G base at +4 relative to the start codon, preceded by an in-frame stop codon. The 5′-untranslated

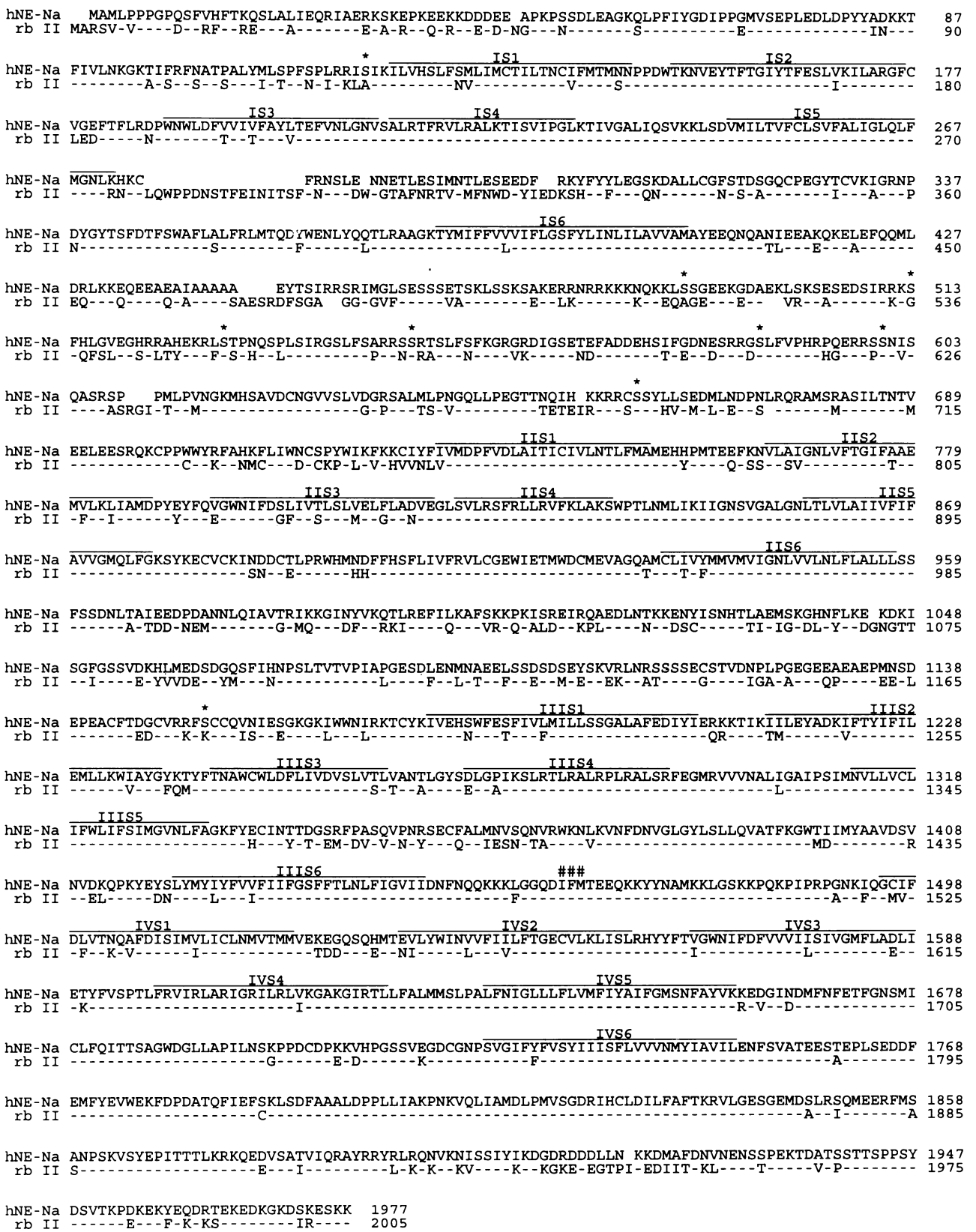

Fig. 1. Primary structure of hNE-Na. The amino acid sequence was deduced from its cDNA and is aligned with the rat brain II sequence (rbII). The suggested locations of the six transmembrane α-helices within each domain are designated by horizontal lines. Potential phosphorylation sites by c-AMP kinase are marked by asterisks. The location of the IFM motif is indicated.

region contains an out-of-frame ATG codon (−8 to −6) which has been shown to be conserved in all previously cloned sodium channel cDNAs (for discussion, see Gellens *et al.*, 1992). Clone pNa18 contains 374 bp of 3′-untranslated sequence including three consensus polyadenylation signals (AATAAA) and a poly(A) tail. The

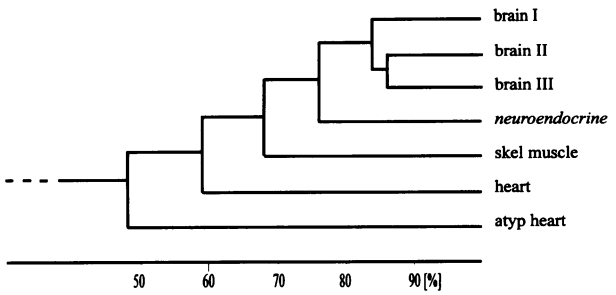

Fig. 2. Phylogenetic tree. Phylogenetic comparison of hNE-Na with sodium channels from rat brain (I, II and III) (Noda *et al.*, 1986; Kayano *et al.*, 1988), rat skeletal muscle μI (Trimmer *et al.*, 1989), human heart hHl (Gellens *et al.*, 1992) and with the human atypical heart channel hNav2.1 (George *et al.*, 1992). The analysis is based on the multiple alignment programs CLUSTAL and TREE (Higgins *et al.*, 1992) using the complete protein sequences. The similarity scores are indicated below the dendrogram.

distance between the most 3′-terminal polyadenylation signal and the poly(A) tail extends 16 bp, indicating the functional relevance of this site.

Hydropathy analysis predicted a transmembrane topology similar to other sodium channels. The channel protein is composed of four domains, each consisting of six transmembrane α-helices and two highly conserved pore-forming short segments (SS1−SS2) (Figure 1).

The transmembrane S4 segments, which form the voltage sensor of the channel, have the same positive charged residues as most other mammalian sodium channels. The number and positions of the arginine and lysine residues within the hNE-Na S4 segments are identical with the brain, heart and skeletal muscle, but not with the atypical heart channel sequence. The latter channel misses several charged residues in domain IV (George *et al.*, 1992).

The primary sequence of hNE-Na conserves the amino acid residues critical for the kinetics of channel activation and inactivation, and potential phosphorylation sites (Catterall, 1994). The hNE-Na sequence contains the IFM motif and the charged residues in the domain III−IV linker identified to be critical for the fast inactivation kinetics of the rat brain II channel (Vassilev *et al.*, 1989; Patton *et al.*, 1992). Furthermore, Ser1479 located carboxy-terminal to the IFM motif may be equivalent to Ser1506 of the rat brain II channel, which is phosphorylated by protein kinase C (Catterall, 1994). Potential cAMP kinase phosphorylation sites are present in the domain I−II linker. It is not clear whether their putative phosphorylation would decrease I_{Na}, as reported for the rat brain II channel, since the amino acid sequence of the I/II linker differs significantly from the rat brain II channel. Other regions which differ significantly from the rat brain II sequence are the extracellular loop between IS5 and the pore region ISS1, the intracellular loop between domain I and II, and the carboxy terminus. The functional significance of these sequence differences has not been examined at present.

Phylogenetic tree

Comparison of hNE-Na with each of the vertebrate sodium channel sequences revealed a high degree of relatedness to this multigene family. The overall amino acid identity is 78–79% to each of the three members of the brain subfamily (Noda *et al.*, 1986; Kayano *et al.*, 1988), 70% to the skeletal muscle μI (Trimmer *et al.*, 1989), 64% to the heart hH1 (Gellens *et al.*, 1992) and 57% to the atypical hNav2.1 sequence (George *et al.*, 1992). Figure 2 shows a dendrogram illustrating the evolutionary relationship among sodium channel sequences. It is obvious that hNE-Na represents an evolutionary link between the channels cloned from skeletal muscle and brain.

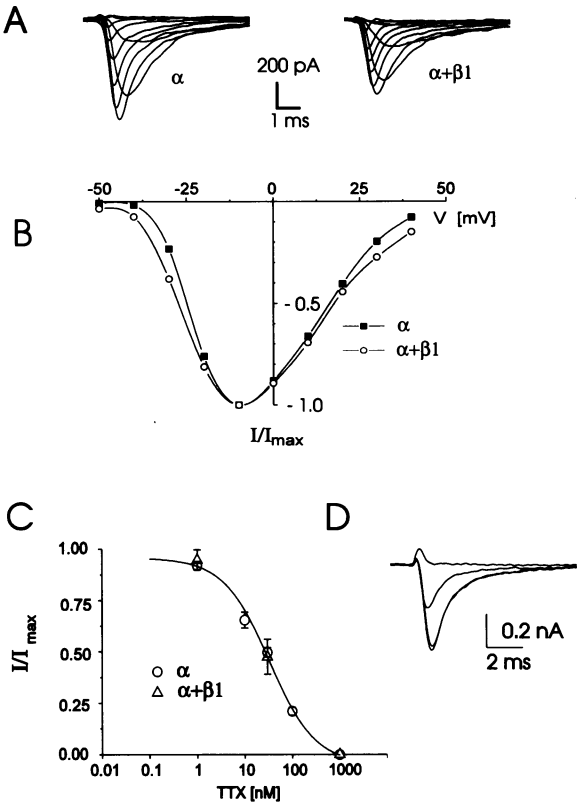

Fig. 3. Sodium currents induced by the hNE-Na α subunit expressed in the absence and presence of the β1 subunit. (**A**) Inward currents activated by depolarizing pulses to membrane potentials between −50 and +40 mV. The traces shown were corrected for leak current obtained at each voltage step in the presence of 1 μM TTX. (**B**) Current–voltage relationships for the same cells as in (A) normalized to maximal inward current. (**C**) Cumulative dose–response curve for TTX. The inhibitory effect of each concentration of TTX was reached within 20 s after changing its bath concentration. Each point is the mean of 5–10 cells. The curves were calculated by fitting the points to the Hill equation with a slope factor of one. (**D**) An example of inward currents activated by 10 ms pulses to −10 mV in the presence of 0, 1, 30 and 1000 nM TTX (from the bottom to the top trace). The cell was transfected with the α subunit.

Electrophysiological recordings

Initial attempts to produce large quantities of a functional expression plasmid failed since bacteria transfected with the 'high-copy' vector pcDNA3 containing the correct hNE-Na sequence did not grow. To overcome this problem, the new 'low-copy' vector pcDNA3a was constructed. Transfected bacteria tolerated this plasmid and produced sufficient quantities of the expression plasmid pNaEx8, which was expressed transiently in the absence and presence of the β1 subunit in HEK 293 cells (Figure 3). The α subunit alone induced rapidly activating and inactivating inward currents (Figure 3A). The threshold for activation was −40 mV and a maximal inward current was reached at −10 mV (Figure 3B). The time to peak and the time

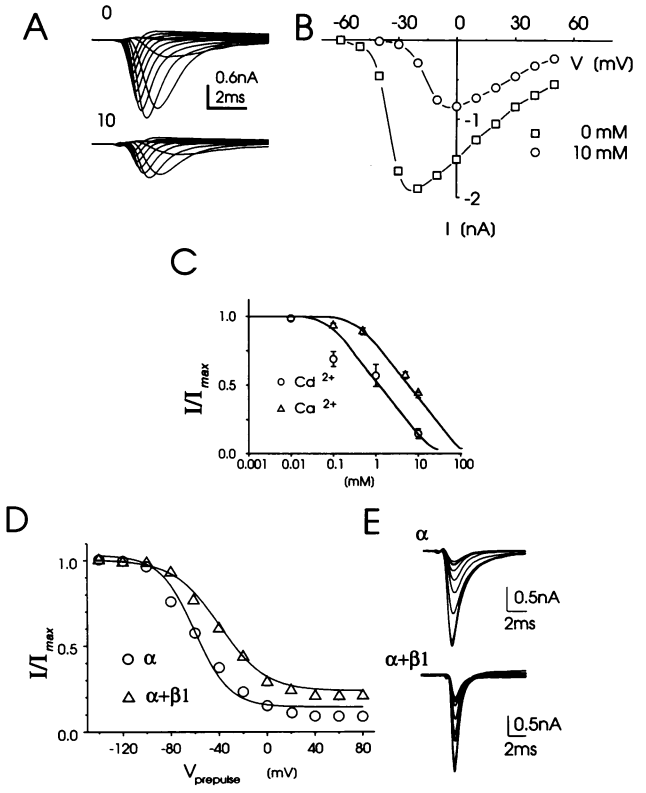

Fig. 4. Block and inactivation of the sodium channel with divalent cations. (**A**) Families of current activated by test pulses ranging from −60 to +50 mV in the absence (○) and presence of 10 mM calcium in the extracellular solution. The calcium-free solution contained 0.1 mM EGTA. (**B**) The corresponding current–voltage relationship in the absence and presence of 10 mM calcium. Same cells as in (A). (**C**) Maximum peak inward current in the presence of the indicated concentrations of calcium or cadmium. Individual I_{max} values were normalized to the values obtained at 0 mM Ca^{2+} or Cd^{2+}. The curves were drawn by eye or fitted by the Hill equation for Ca^{2+} and Cd^{2+}, respectively. (**D**) Steady-state inactivations for the α subunit and the co-expressed α+β1 subunit in the absence of Ca^{2+}. The experimental points were fitted to the Boltzmann equation. (**E**) Examples of families of currents registered during the test pulse in an α subunit (above) and an α+β1 subunit (bottom) expressing cell. The pre-pulses varied from −120 to +80 mV with a step of 20 mV; same cells as in (D).

constant for current decay decreased with depolarizing pulses to positive membrane potentials. None of these characteristics was affected significantly when the β1 subunit was co-expressed (Figure 3A and B, but see Figure 4D). The average sodium current I_{Na} density was 65 ± 9 pA/pF (n = 44) and 66 ± 17 pA/pF (n = 9) in the absence and presence of β1 subunit, respectively. The inward currents elicited by each combination were blocked rapidly and reversibly by TTX (Figure 3C and D). The experimental points were fitted to the Hill equation with a factor of one, indicating non-cooperative binding of TTX to a single site. The IC_{50} values obtained from these fits were 24.5 and 26.0 nM for the α subunit alone and the α and β1 subunit complex, respectively. These values closely match those reported for rat sodium channel II (Noda *et al.*, 1989).

The TTX-sensitive sodium channels are usually blocked poorly by divalent cations, whereas TTX-insensitive channels are blocked by micromolar concentrations of cadmium (Satin *et al.*, 1992). Indeed, the sodium current through the expressed α subunit in the absence and presence of the β1 subunit was suppressed by both Cd^{2+} and Ca^{2+} at millimolar concentrations (Figure 4A–C). Both cations shifted the current–voltage relationships of the sodium current by up to 25 mV to more depolarized potentials in a concentration-dependent manner. The dose–response curves constructed from the maximal peak inward currents yielded IC_{50} values of 1.1 and 6.8 mM for Cd^{2+} and Ca^{2+}, respectively (Figure 4C).

The expressed α subunit inactivated under steady-state condition at negative membrane potentials with a $V_{0.5}$ value of −60.5 ± 1.6 mV (n = 15) (Figure 4D). The β1 subunit shifted the steady-state inactivation curve by 20 mV towards the more depolarized potentials with a $V_{0.5}$ value of −39.6 ± 1.7 mV (n = 6) in the absence of calcium (Figure 4D), but not in its presence (not shown). About 15% of the sodium current was not inactivated at positive potentials in the absence of calcium, whereas almost 100% inactivation was observed in the presence of calcium (not shown). Inspection of individual traces showed that the inactivation was slightly faster in the presence than in the absence of the β1 subunit (Figure 4E). The inactivation traces could be fitted by monoexponential curves yielding inactivation time constants of 1.3 ± 0.1 ms (n = 15) and 0.83 ± 0.07 ms (n = 6) for α and α plus β1 subunit-expressing cells, respectively.

Previously, it was shown that TTX-sensitive action potentials could be elicited in chromaffine cells (Biales *et al.*, 1976) and C-cells (Biagi *et al.*, 1992; Scherübl *et al.*, 1993). We tested, therefore, whether or not action potentials could be elicited in HEK cells which expressed the hNE-Na channel, since HEK 293 cells have relatively large K^+ currents. The cells were dialyzed with a potassium-containing pipette solution and had a resting membrane potential between −35 and −45 mV. Over 50% of the sodium channels were inactivated at these membrane potentials (see Figure 4D). The release from inactivation was induced by injecting −30 pA current, which lowered the membrane potential to ~ −80 mV. Action potentials were then initiated by current pulses between −10 and +17 pA (Figure 5). The voltage threshold for firing action potential was at ~ −40 mV. Only cells with high expression levels of hNE-Na, i.e. I_{Na} amplitudes in the nanoampere range, generated action potentials. The cells with I_{Na} between 200 and 800 pA showed an active electrical response upon current injection, but were never able to produce an overshoot response (not shown). Only a passive electrical response was obtained with non-transfected wild-type HEK 293 cells.

Tissue distribution of hNE-Na

Poly(A) RNA was isolated from various tissues and analyzed by Northern blot hybridization (Figure 6). The hNE-Na probe hybridized with transcripts of 7.0 and 9.4 kb in a C-cell carcinoma and in the clonal hMTC cell line (Figure 6A). These signals were visible after a 2 day exposure on the film. Extending the exposure time to 9 days did not indicate a specific transcript in pig or bovine thyroid gland, in rat brain or pancreas, or human pituitary (Figure 6A). The 9.4 kb transcript was also identified in mRNA from bovine adrenal gland, but not in mRNA from rat heart, rabbit kidney, colon, testis, liver, or bovine testis, diencephalon or pineal gland, although exposure time was extended to 8 days (Figure 6B). The

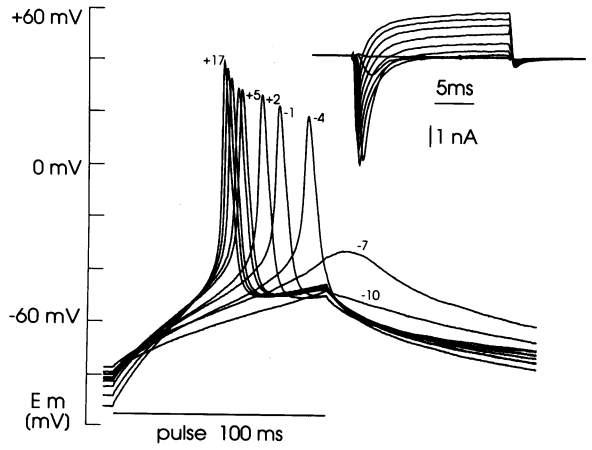

Fig. 5. Cells expressing hNE-Na can generate action potential. The cell was hyperpolarized to ~−80 mV by injecting −30 pA holding current. The membrane potential trajectories were evoked by current pulses with the amplitude increasing by 3 pA/step. The first current pulse was to −10 pA. The number above individual traces is the corresponding clamp current in pA. Inset: The family of inward and outward currents measured under the voltage–clamp conditions in the same cell, depolarized from −80 mV to potentials between −40 and +50 mV using the same extra- and intracellular solutions with a step of 10 mV.

same hNE-Na-specific probe hybridized specifically with human genomic DNA, suggesting that hNE-Na was derived from an as yet unidentified gene (not shown).

Together with the sequence comparison, these Northern analyses indicated that hNE-Na was specifically expressed in neuroendocrine tissues. To further support this possibility, the presence of hNE-Na mRNA in thyroid tissue was tested by reverse transcription-polymerase chain reaction (RT-PCR) amplification. These experiments were carried out with poly(A) RNA from bovine tissues to avoid potential contaminations from the human clones. Bovine cerebellum and adrenal gland were included as negative and positive controls, respectively. The amplification yielded a specific product with poly(A) RNA from thyroid and adrenal gland (Figure 6C). Sequencing of the subcloned DNA fragment demonstrated that the amplified DNA fragment contained part of the sequence of the bovine NE-Na channel, which was 93% identical with the human sequence.

Discussion

Voltage-sensitive sodium channels form a multigene family with at least seven structurally distinct isoforms currently identified in rat brain, skeletal muscle and heart. There are several lines of evidence that a similar number of tissue-specifically expressed sodium channels are present in human. We have identified the transcript of a novel human sodium channel. The hNE-Na sequence is not the human homolog of any previously cloned cDNA from rat. The degree of primary structure identity that exists between the genes of different species, i.e. rat and human, typically exceeds >90% overall amino acid identity (Gellens *et al.*, 1992). The highest degree of sequence identity exists between hNE-Na and rat brain II, which is 79%.

A phylogenetic analysis of the sodium channel gene

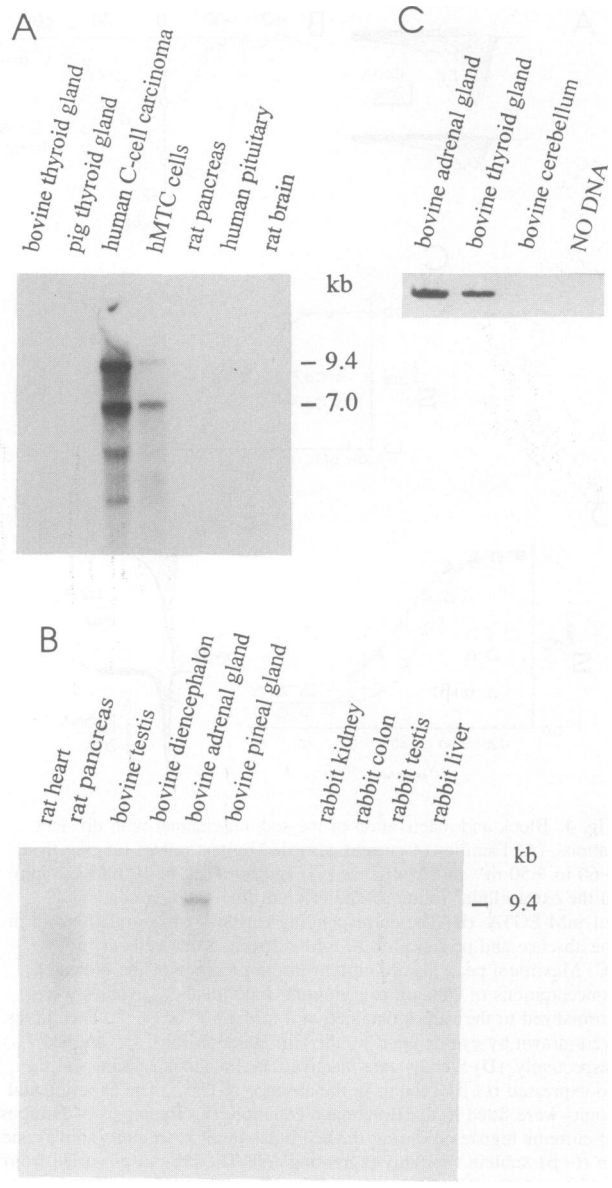

Fig. 6. Northern and RT-PCR analysis of hNE-Na. (**A** and **B**) Northern blot hybridization of hNE-Na transcripts in different tissues and in hMTC cells. The amount of poly(A) RNA was 10 μg/slot. Autoradiographic exposure was 2 days for (A) and 9 days for (B). (**C**) Tissue distribution of hNE-Na by RT-PCR. Reverse transcription reactions using poly(A) RNA extracted from the indicated tissues were used in the PCR with unique oligonucleotide primers directed against C-terminal and 3′-untranslated sequences. The identity of the amplified DNA with hNE-Na was established by subcloning and sequencing.

family published recently (Strong *et al.*, 1993) demonstrates that a series of duplications generated the different mammalian genes. The dendrogram presented here is in agreement with this tree and shows the same branching pattern. It includes the sequences of hNE-Na and of the atypical sodium channel expressed in heart and uterus (George *et al.*, 1992). This calculation indicates that hNE-Na branches off from the common ancestor of the skeletal muscle and the brain subfamily.

The electrophysiological data show that the hNE-Na expressed in HEK 293 cells has a fast time course for both activation and inactivation, typical for the native channels. The channel has a high and low sensitivity to

TTX and divalent cations, respectively. The TTX sensitivity is similar to that reported for the native sodium current of bovine chromaffine cells (Fenwick *et al.*, 1982), of human (Biagi *et al.*, 1992) and rat (Scherübl *et al.*, 1993) medullary thyroid carcinoma cells. Sequence comparison with the TTX-sensitive brain and skeletal muscle isoforms shows that hNE-Na has the aromatic residue Tyr 362, which confers the high sensitivity for TTX block in the rat brain II channel (Satin *et al.*, 1992). The expressed channel was able to induce action potentials in HEK 293 cells. This indicates that the channel may physiologically generate action potentials in neuroendocrine cells.

If expressed in oocytes, some sodium channel α subunits require co-expression of the β1 subunit to yield normal fast inactivation kinetics and a high current level (see Catterall, 1994). The same sodium channel α subunits showed regular kinetics when expressed in mammalian cells (West *et al.*, 1992). The potential effect of the co-expression of the β1 subunit was not studied in these latter experiments. The results of this study directly confirm that the hNE-Na α subunit does not require a β1 subunit either to reproduce the kinetics of the native channel, or to reach a high current density level. The β1 subunit had some discrete effects on the kinetics of the expressed hNE-Na channel when the experiments were carried out in the absence of external calcium. The β1 subunit speeded up slightly the inactivation time course and apparently shifted the steady-state inactivation curve to depolarized membrane potentials in the absence of extracellular calcium. This shift is the opposite to that observed with some sodium channels expressed in *Xenopus* oocytes (Isom *et al.*, 1992; McClatchey *et al.*, 1993). These results suggest that the potential function of the β1 subunit may be related to the inactivation kinetics in mammalian cells.

As reviewed by Mandel (1992), the expression of individual sodium channel genes is regulated tightly in terms of cell specificity and development. In line with this notion, hNE-Na is exclusively expressed in some cells of the neuroendocrine system. Northern blots indicated that the hNE-Na gene is highly expressed in cultured C-cells and a C-cell carcinoma. The hNE-Na transcript was not detected in the poly(A) RNA derived from thyroid gland. This apparent discrepant expression is due to the very low number of C-cells present in the thyroid gland, where they comprise <0.1% of the total cell number (Biagi *et al.*, 1992). This interpretation was confirmed by RT-PCR analysis which indicated that the mRNA of NE-Na was present in bovine thyroid and adrenal gland, but not in cerebellum. Additionally, hNE-Na may be less expressed in adult cells than in rapidly growing C-cells. Parafollicular C-cells of the thyroid gland are derived from the neural crest and secrete calcitonin in response to elevated extracellular Ca^{2+} concentrations. C-cells have spontaneous action potentials which are completely blocked by TTX (Biagi *et al.*, 1992; Scherübl *et al.*, 1993), suggesting that the cloned hNE-Na channel may participate physiologically in the secretion process.

Northern and RT-PCR analyses also showed expression of hNE-Na in the adrenal gland. As demonstrated by Biales *et al.* (1976), adrenal chromaffin cells are capable of generating action potentials in response to depolarizing currents or to direct application of acetylcholine. These action potentials are considered to be generated by a mechanism involving sodium channels. Northern blot signals of similar size were detected in the mRNA derived from peripheral nervous tissue (Beckh, 1990) and pheochromocytoma cells (D'Arcangelo *et al.*, 1993), potentially suggesting that the hNE-Na channel may also be expressed in these tissues.

In conclusion, a common characteristic of the cells expressing hNE-Na is their involvement in secretory activity, their ability to generate spontaneous action potentials and their origin from the neural crest. It is, therefore, likely that hNE-Na is a neuroendocrine-specific sodium channel.

Materials and methods

RNA isolation

Poly(A) RNA from hMTC cells was purified using the Fast Track Kit (Invitrogen). Total RNAs from a human C-cell carcinoma, from rat brain, heart and pancreas, from bovine testis, thyroid gland, adrenal gland, pineal gland and diencephalon, from rabbit kidney, colon, testis and liver, and pig thyroid gland was isolated by the guanidinium thiocyanate method and poly(A) RNA was separated by oligo(dT) cellulose chromatography. Pituitary gland poly(A) RNA was obtained from Clontech.

Library screening and construction of full-length cDNA

A size-selected oligo(dT)-primed hMTC cell cDNA library constructed in pSPORT1 vector (Gibco BRL Life Technologies) was screened with a cDNA probe derived from the rat brain sodium channel II sequence (*Sst*I 3930–*Hin*dIII 5449) (Noda *et al.*, 1986). Screening of the library yielded a partial clone (pNa18) encoding domains II, III and IV of a voltage-activated sodium channel [nucleotides (nt) 1309–5931 and 374 bp of the 3′-untranslated region]. Sequence analysis revealed that pNa18 has a one nucleotide deletion (nt 5323, W1775). The corresponding cDNA region was amplified by RT-PCR using hMTC poly(A) RNA, the fragments were cloned in pT7Blue (Novagen). Sequence analysis of six clones demonstrated that only pNa18 contained the deletion. The frameshift mutation was corrected later in the full-length construct (pNaEx8) using one of the PCR-generated clones.

A second cDNA library was primed using the antisense oligonucleotide 5′-GCA TCT CCC TTT TCC TC-3′, which corresponds to residues 492–497 and a random hexanucleotide primer. This cDNA library was screened with a 150 bp 5′-terminal fragment of pNa18. Several independent clones were identified; one of them, pNa3a, containing the 5′-untranslated region and nt 1–1490 of the open reading frame was used for construction of a full-length cDNA (pNaEx8).

Several attempts to construct a full-length recombinant plasmid in the high-copy number vectors pSPORT (Gibco BRL Life Technologies) and pcDNA3 (Invitrogen) failed. To circumvent these cloning problems, we used pBR322 for further experiments. For transient expression of pNaEx8 in eukaryotic host cells, the pcDNA3 vector (Invitrogen) was modified by replacing the *Bsm*I (nt 3200)–*Pvu*I (nt 4894) fragment containing the ColE1 origin with the corresponding *Bsm*I (nt 1353)–*Pvu*I (nt 3733) fragment of pBR322. The full-length cDNA was cloned into this modified pcDNA3a vector: the 5′- and 3′-untranslated regions were removed, and a consensus sequence for the initiation of translation was inserted by PCR standard techniques. The 1408 bp fragment (nt 1–1408 *Sst*I), the 696 bp fragment (*Sst*I 1409–*Bst*XI 2105) and the 3828 bp fragment (*Bst*XI 2106–nt 5934) were ligated with pcDNA3a to yield the recombinant plasmid pNaEx8. The nucleotide sequence of hNE-Na has been submitted to the EMBL sequence database and is available under accession number X82835.

Calculation of phylogenetic tree

A phylogenetic analysis is based on the multiple alignment programs CLUSTAL and TREE (Higgins *et al.*, 1992). For construction of alignment, the complete amino acid sequences of seven mammalian genes was used (Noda *et al.*, 1986; Kayano *et al.*, 1988; Trimmer *et al.*, 1989; Gellens *et al.*, 1992; George *et al.*, 1992).

Northern blot and RT-PCR analysis

Poly(A) RNA was fractionated on a 1.2% agarose gel, transfered to Biodyne nylon membranes (Pall) and hybridized under high stringency

with a cDNA probe. The probe used was a 706 bp random primed labeled fragment corresponding to the intracellular loop between domains I and II (nt 1557–2263).

Poly(A) RNA was reverse transcribed using oligo(dT) primers. PCR amplification (30 cycles) used unique oligonucleotides directed against C-terminal coding and 3′-untranslated sequences. Reaction products were electrophoresed, eluted and cloned in pUC18. Sequence analysis confirmed the identity of the amplified DNA fragments. The integrity of the first-strand cDNA which did not yield a specific amplification product was examined by positive control PCR reactions. Amplification products were visualized by ethidium bromide staining and digitally recorded.

PCR amplification of the sodium channel β1 subunit

Oligonucleotide primers (adapter primer 1 containing *Hin*dIII and *Eco*RV restriction sites and a consensus sequence for initiation of translation: 5′-ATC TAA GCT TGA TAT CGC CGC CAC CAT GGG GAG GCT GCT GGC CTT A-3′; and adapter primer 2 containing a *Bam*HI restriction site: 5′-CGG GAT CCC TAT TCG GCC ACC TGG ACG CCC G-3′) complementary to nucleotides 98–118 and 732–754, respectively, of the human β1 subunit cDNA (McClatchey *et al.*, 1993) were used for PCR amplification on hMTC poly(A) RNA. The PCR product was cloned in pcDNA3 (Invitrogen) to yield the recombinant plasmid pNaβ1 and was sequenced on both strands.

Transfection of HEK 293 cells and electrophysiological recordings

HEK 293 cells were transiently transfected with either pNaEx8 alone or together with pNaβ1 (1:1 mass ratios) using the calcium phosphate method.

I_{Na} was measured at room temperature using whole-cell patch-clamp technique. The bath solution contained (in mM): 150 NaCl, 2 KCl, 2 $CaCl_2$, 1 $MgCl_2$, 10 HEPES, 10 glucose, pH 7.4 (NaOH). The pipette solution contained (in mM): 120 CsCl, 2 $MgCl_2$, 10 EGTA, 10 TEACl, 10 HEPES, pH 7.4 (CsOH). When filled with this solution, typical pipette resistance ranged from 1.7 to 1.9 MOhm. For the current–clamp experiments, the bath solution contained (in mM): 115 NaCl, 2 $CaCl_2$, 2 $MgCl_2$, 5 KCl, 5 HEPES, pH 7.4 (NaOH) and the pipette solution contained (in mM): 115 KCl, 1 EGTA, 4 $MgCl_2$, 5 HEPES, pH 7.4 (KOH). Cell capacitance ranged from 10 to 50 pF. Pipette and membrane capacitances were neutralized by built-in circuits. Series resistance ranged between 4 and 10 MOhm, and was compensated by 10–40%. I_{Na} was elicited by applying 10 ms depolarization pulses from a holding potential of −100 to −10 mV at 0.2 Hz. Steady-state inactivation curves were determined by using a 2 s pre-pulse to potentials between −140 and +80 mV, followed by a 10 ms return to −100 mV, followed by a 10 ms long test pulse to −10 mV. Although a significant endogenous I_{Na} was not observed in non-transfected wild-type cells, only the cells with a current density >20 pA/pF were analyzed. Values are given as mean ± SEM with the number of cells in parentheses. Significance was tested using paired or non-paired Student's *t*-test.

Acknowledgements

We thank Mrs Erhard and Mrs Mayr for expert technical assistance. We thank Dr Hescheler for providing hMTC cells and Dr Raue for human C-cell carcinoma. The work was supported by grants from the Deutsche Forschungsgemeinschaft and Fond der Chemie.

References

Beckh,S. (1990) *FEBS Lett.*, **262**, 317–322.
Beckh,S., Noda,M., Lubbert,H. and Numa,S. (1989) *EMBO J.*, **8**, 3611–3616.
Biagi,B.A., Mlinar,B. and Enyeart,J.J. (1992) *Am. J. Physiol.*, **263**, C986–C994.
Biales,B., Dichter,M. and Tischler,A. (1976) *J. Physiol.*, **262**, 743–753.
Catterall,W.A. (1994) *Renal Physiol. Biochem.*, **17**, 121–125
D'Arcangelo,G., Paradiso,K., Shepherd,D., Brehm,P., Halegoua,S. and Mandel,G. (1993) *J. Cell Biol.*, **122**, 915–921.
Fenwick,E.M., Marty,A. and Neher,E. (1982) *J. Physiol.*, **331**, 599–635.
Gautron,S., Dos Santos,G., Pinto-Henrique,D., Koulakoff,A., Gros,F. and Berwald-Netter,Y. (1992) *Proc. Natl Acad. Sci. USA*, **89**, 7272–7276.
Gellens,M.E., George,A.L.,Jr, Chen,L., Chahine,M., Horn,R., Barchi,R.L. and Kallen,R.G. (1992) *Proc. Natl Acad. Sci. USA*, **89**, 554–558.
George,A.L.,Jr, Knittle,T.J. and Tamkun,M.M. (1992) *Proc. Natl Acad. Sci. USA*, **89**, 4893–4897.
Higgins,D.G., Bleasby,A.J. and Fuchs,R. (1992) *Comput. Appl. Biosci.*, **8**, 189–191.
Isom,L.L., Dejongh,K.S., Patton,D.E., Reber,B.F.X., Offord,J., Charbonneau,H., Walsh,K., Goldin,A. and Catterall,W.A. (1992) *Science*, **256**, 839–842.
Isom,L.L., DeJongh,K.S. and Catterall W.A. (1994) *Neuron*, **12**, 1183–1194.
Kallen,R.H, Cohen,S.A. and Barchi,R.L. (1994) *Mol. Neurobiol.*, **7**, 383–428.
Kayano,T., Noda,M., Flockerzi,V., Takahashi,H. and Numa, S. (1988) *FEBS Lett.*, **228**, 187–194.
Mandel,G. (1992) *J. Membr. Biol.*, **125**, 193–205.
McClatchey,A.I., Cannon,S.C., Slaugenhaupt,S.A. and Gusella,J.F. (1993) *Hum. Mol. Genet.*, **2**, 745–749.
Noda,M., Ikeda,T., Kayano,T., Suzuki,H., Takeshima,H., Kurasaki,M., Takahashi,H. and Numa,S. (1986) *Nature*, **320**, 188–192.
Noda,M., Suzuki,H., Numa,S. and Stühmer,W. (1989) *FEBS Lett.*, **259**, 213–216.
Patton,D.E., West,J.W., Catterall,W.A. and Goldin,A.L.(1992) *Proc. Natl Acad. Sci. USA*, **89**, 10905–10909.
Satin,J., Kyle,J.W., Chen,M., Bell,P., Cribbs,L.L., Fozzard,H.A. and Rogart,R.B. (1992) *Science*, **256**, 1202–1205.
Scherübl,H., Kleppisch,T., Zink,A., Raue,F., Krautwurst,D. and Hescheler,J. (1993) *Am. J. Physiol.*, **264**, E354–E360.
Strong,M., Chandy,K.G. and Gutman, G.A. (1993) *Mol. Biol. Evol.*, **10**, 221–242.
Stühmer,W. (1993) *Cell Physiol. Biochem.*, **3**, 277–282.
Trimmer,J.S. *et al.* (1989) *Neuron*, **3**, 33–49.
Vassilev,P.M., Scheuer,T. and Catterall,W.A. (1989) *Proc. Natl Acad. Sci. USA*, **86**, 8147–8151.
West,J.W., Scheuer,T., Maechler,L. and Catterall,W.A. (1992) *Neuron*, **8**, 59–70.

Received on November 9, 1994; revised on December 22, 1994